ASIAN JOURNAL OF PHARMACEUTICAL AND CLINICAL RESEARCH

INNOVARE ACADEMIC SCIENCES
Knowledge to Innovation

Vol 19, Issue 1, 2026

Online - 2455-3891
Print - 0974-2441

Research Article

DESIGN, SYNTHESIS, AND ANTIMYCOBACTERIAL EVALUATION OF NOVEL PYRROLE-OXADIAZOLE MOLECULAR HYBRID AGAINST MYCOBACTERIUM TUBERCULOSIS

GANESH D MOTE[1,2]*, MAHESH G SARALAYA[3]

[1]Department of Pharmaceutical Chemistry, Annasaheb Dange College of B. Pharmacy, Ashta, Maharashtra, India. [2]Department of Pharmaceutical Chemistry, Ashokrao Mane College of Pharmacy, Pethvadgaon, Maharashtra, India. [3]Department of Pharmacology, Annasaheb Dange College of B. Pharmacy, Ashta, Maharashtra, India.
***Corresponding author: Ganesh D Mote; Email: mote.ganeshadcbp@gmail.com**

Received: 20 September 2025, Revised and Accepted: 06 November 2025

ABSTRACT

Objective: To enhance the potency of susceptible *Mycobacterium tuberculosis* (MTB) and create novel derivatives for multidrug-resistant tuberculosis with a molecular hybrid of pyrrole with oxadiazole.

Methods: A number of pyrrole-ligated oxadiazole molecular hybrid derivatives have been developed and produced in response to the bioisosteric similarities between isoniazid and pyrazinamide. Fourier transform infrared spectral data, mass spectrometry, and nuclear magnetic resonance were used to identify the target chemicals. The toxicity of the chosen ligands was assessed using human dermal fibroblast cell lines, and the *in vitro* Microplate Blue Alamar assay for antitubercular action of all the prepared compounds against the strain MTB H37Rv was assessed.

Results: Every developed drug exhibited MTB inhibition, with a minimum inhibitory concentration (MIC) ranging from 3.12 to 50 μM. OP3 was the most effective MTB inhibitor among the drugs evaluated (MIC=3.12 μM).

Conclusion: The current study's findings indicate that the majority of the synthesized compounds exhibit an adequate range of molecular characteristics and are sensitive to MTB.

Keywords: Molecular hybrid of pyrrole with oxadiazole, Antitubercular agent, Microplate Blue Alamar assay, Molecular docking, Lipinski's rule of five.

DOI: http://dx.doi.org/10.22159/ajpcr.2026v19i1.56941. Journal homepage: https://innovareacademics.in/journals/index.php/ajpcr

INTRODUCTION

Globally, tuberculosis (TB) is the most common and deadly infectious illness. *Mycobacterium tuberculosis* (MTB), a slow-growing bacterium, is the cause of TB. The World Health Organization estimates that 1.9 million TB fatalities and 11.7 million new TB cases occurred in 2023. Furthermore, southern Asia, Pacific countries (West), and African countries account for almost 70% of all TB cases worldwide [1]. Isoniazid, pyrazinamide, and rifampicin must be taken for 120 days as part of the widely employed TB cure therapy, i.e., direct observed treatment, which is followed by another 120 days of isoniazid and rifampicin treatment [2,3]. MTB has developed resistance to several first-line medications [4]; therefore, it is necessary to identify new and improved therapeutic candidates for treatment. Academics and industry have taken an interest in pyrrole and oxadiazole. Antitubercular [5], antibacterial [6], anticancer [7,8], antioxidant [9], and antifungal [10] activities are only a few of its intriguing biological qualities. Based on the effect, resistance, and multidrug therapy of antitubercular medications like pyrazinamide, isoniazid, rifampicin, ethambutol, streptomycin, and para-aminosalicylic acid, we have designed with pyrrole and oxadiazole moieties to reduce multidrug resistance (MDR) TB, potentially impacting the mycobacterial cell wall [5]. Pyrrole-based antitubercular agents exert their activity mainly by targeting key enzymes in MTB – including enoyl-ACP reductase and MMA4, thereby interrupting essential metabolic and cell wall biosynthesis processes crucial for bacterial survival. The hybridization aims to yield synergistic effects, overcome resistance, and improve pharmacokinetics by targeting methoxy mycolic acid synthase 4 (MMA4), which is responsible for the synthesis of the bacterial cell wall by transferring a methyl group for acetylation. Hence, molecular hybrid blocks the synthesis of the cell wall by avoiding the transfer of the methyl group for acetylation. In addition, allylic carbonyl derivatives of pyrrole with oxadiazole have shown various biological properties with drug-like effect, such as antibacterial, antifungal, antitubercular, and anticancer properties, and are commonly employed as scaffolds in biology-oriented synthesis [11,12].

Considering the aforementioned observations, we synthesized target compounds in response to the varied pharmacological activities of these pharmacophores, assuming that their hybridization in a single structural entity might produce novel heterocyclic compounds with notable synergistic antitubercular properties. Structure–activity relationship (SAR) investigations to construct a variety of novel molecular hybrid compounds combining pyrrole with oxadiazole in an attempt to find new and potent antitubercular medicines. Therefore, a series of new pyrroles with oxadiazole derivatives including allylic carbonyl [11,12] molecular hybrids were developed based on SAR study and prepared using synthetic routes shown in Fig. 1 to generate prospective antitubercular medicines (Fig. 2). The current work employed human dermal fibroblast cell lines for toxicity tests all the compounds are evaluated for in vitro antimycobacterial efficacy against MTB H37Rv and compared with the standard. Pyrrole and oxadiazole complexation is a strong contender for MMA4 enzyme targeting for bactericidal effects. Our current work is focused on the molecular docking and in-silico construction of a new molecular hybrid for antitubercular actions that combines pyrrole with oxadiazole derivatives for a synergistic multifunctional mechanism (multi-target action), reduced resistance potential compared to single pharmacophores, improved solubility, stability, and pharmacokinetics.

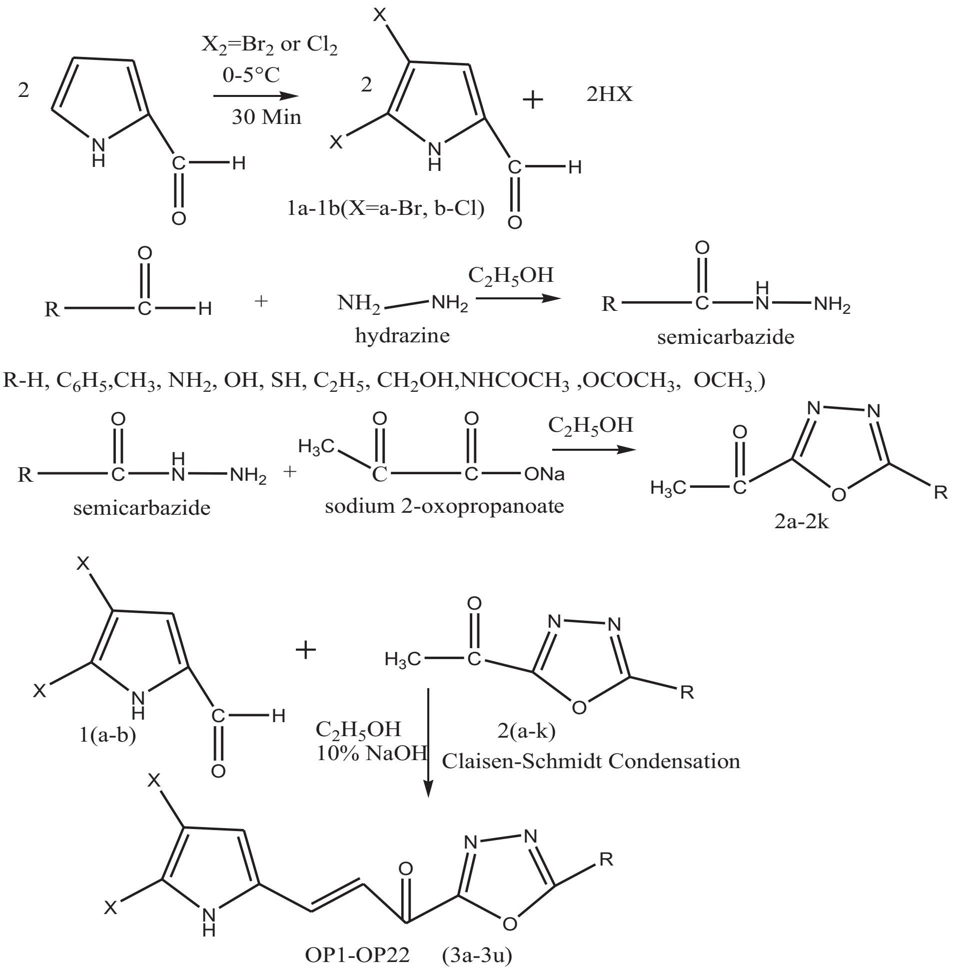

3a-3k(X-Br,R-H, C_6H_5,CH_3, NH_2, OH, SH, C_2H_5, CH_2OH,$NHCOCH_3$,$OCOCH_3$, OCH_3.)(OP_1,3,5,7,9,11,13,15,17,19,21)

3l-3u(X-Cl,R-H, C_6H_5,CH_3, NH_2, OH, SH, C_2H_5, CH_2OH,$NHCOCH_3$,$OCOCH_3$, OCH_3.)(OP_2,4,6,8,10,12,14,16,18,20,22)

Fig. 1: Synthetic scheme of the molecular hybrid of pyrrole with oxadiazole with reagent conditions

METHODS

Synthesis of molecular hybrid of pyrrole with oxadiazole derivatives (OP1–OP22)

Ten percent sodium hydroxide (3 mL) was utilized as a solvent after equimolar volumes of 4, 5, substituted pyrrole carbaldehyde (1a-1b) (20 mmol) and substituted 2-oxadiazole methanone (2a-2k) (20 mmol) [13-16] were dissolved in ethanol. After that, the reaction assembly was heated for 120 min at 85°C. The resultant mixture cooled when the reaction was finished, as determined by thin-layer chromatography (TLC). After being suction-filtered, the precipitate was cleaned using cooled ether and ethanol. Several spectroscopic methods were used to manufacture and study the structures of the target compounds 3a-3u (OP1–OP22).

Microplate Blue Alamar (MABA) assay for antimycobacterial evaluation

The MABA assay [17] was used to measure antitubercular activity. The sterile deionized water was filled into each of the outside perimeter wells of the sterile 96-well plate to reduce evaporation during incubation. The broth Middlebrook (7H9) 100 μL was added to each of the 96-well plates, and the serial standard concentrations of synthesized compounds were prepared in a 10 mL volumetric flask in the concentration range 0.01–20.0 μg/mL. Each concentration solution was added to the bacterial solution, having an inoculum size of 5×10^5. Standard isoniazid, ciprofloxacin, and pyrazinamide were taken as the reference standard. The control solution was also prepared without a drug for the negative control. The plates were incubated for 5 days at 37°C after being covered and parafilm-sealed. After this, the tubes were filled with 25 μL of a freshly prepared mixture of Almar Blue reagent and 10% Tween 80 in a 1:1 proportion, and it was kept for incubation for at least 24 h. A development of pink color in the well was the indicator of antimycobacterial action, whereas a blue color indicated resistance to antimycobacterial drugs. The color pink intensity was checked on ultraviolet spectroscopy at 570 nm. The lowest medication concentration that changed the color from blue to pink was known as the minimum inhibitory concentration (MIC) [18,19].

In vitro cytotoxicity assay

The methylthiazolyldiphenyl-tetrazolium bromide (MTT) assay technique was implemented for assessing the toxicity testing of certain compounds. The cytotoxicity test using the MTT reagent was employed for assessing the percentage of viability of tuberculous cells (CGD-1 kit, Sigma–Aldrich). 96-well plates (Perkin Elmer Spectra Plate) were seeded with fibroblast cells of human dermatitis (1000 cells/well). Following a 24-h incubation period, the media were swapped out for 100 μL of media made using pyrrole and oxadiazole hybrids (OP1–

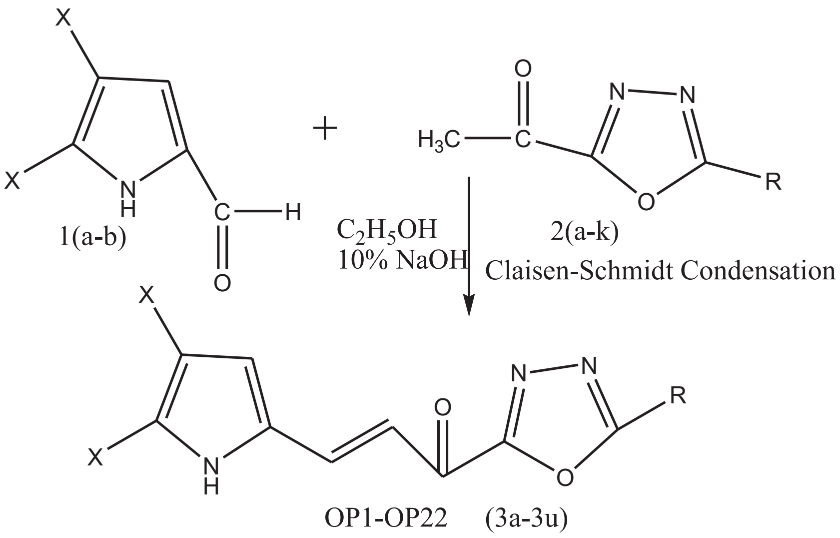

3a-3k(X-Br,R-H, C_6H_5,CH_3, NH_2, OH, SH, C_2H_5, CH_2OH,$NHCOCH_3$,$OCOCH_3$, OCH_3.)(OP_1,3,5,7,9,11,13,15,17,19,21)

3l-3u(X-Cl,R-H, C_6H_5,CH_3, NH_2, OH, SH, C_2H_5, CH_2OH,$NHCOCH_3$,$OCOCH_3$, OCH_3.)(OP_2,4,6,8,10,12,14,16,18,20,22)

Fig. 2: Complexation scheme for the synthesis of a molecular hybrid of pyrrole with oxadiazole

OP22) at 2.5, 10, 25, 50, and 100 μg/mL. After treatment, the medium was discarded from each well and replaced with a fresh medium that contained 10% of the culture volume of the MTT solution. The medium was then incubated for 3 h at 37 °C until a purple formazan product appeared.

A microplate sensor recorder was adopted to measure the absorbance at 570 and 690 nm; after that, formazan product was obtained, and it was dissolved in acidified isobutanol. Absorbance at 570 nm was deducted from background absorbance at 690 nm [20,21].

Molecular docking studies

The structures of all the designed compounds were drawn using the ChemDraw Chem2D Ultra software and saved in.mol format. The structures of all 22 new chemical entities were optimized using force field analysis, and the energies of all the designed compounds were minimized. The structures were converted into the open Babel platform present in PyRx. Target receptor having pdb id 3HA7 (Methoxy mycolic acid Synthase 4) was downloaded from RCSB site The receptor structure was uploaded to Biovivo Discovery Studio, and water molecules, non-standard residues, and ligands were removed from the receptor. Polar hydrogens were added to the receptor for favorable hydrogen bonding and saved in the form of .pdb. The prepared receptor structure was uploaded to PyRx and converted into .pdbqt form. The Ligand receptor was uploaded to PyRx. The binding site was defined by setting a proper grid box with proper dimensions at X, Y, and Z to cover the active site. Receptor and designed molecules uploaded through Auto-Dock Vina and docked on the software for interaction. The start button was clicked, the grid box was selected at maximum, and the docking analysis was submitted. The binding energy or docking score was obtained in CSV form, which was in negative energy. Potency was determined based on the negative score. The more negative the score, the greater the potency. The best docking pose was selected based on the model, and the first model was saved as pose 1 of the docked ligand. Pose 1 of the docked ligand was saved in.pdb format. Pose 1 was opened in the Biovivo discovery studio, and the receptor was in the Biovivo discovery studio. Clicked on analyze and “Receptor-Ligand Interaction” and hydrogen bonds, hydrophobic interaction, and electrostatic forces were visualized [22-24].

RESULTS

Synthesis and spectral data

All the synthesized compounds were characterized for structure confirmation, and its elucidation by Fourier Transform Infra-Red (FTIR) Spectroscopy, Make: Bruker, Model: Alpha-II, Nuclear Magnetic Resonance (NMR) Spectroscopy, Make: Bruker, Model: AV-III, 400 MHz, Mass Spectroscopy, Make: Agilent, Model: LC-MSD-iQ LCMS

(E)-3-(4,5-dibromo-1H-pyrrol-2-yl)-1-(1,3,4-oxadiazolyl)prop-2-en-1-one(OP1)

Percentage of product yield: 75%; M.P(°C): 142–144; IR-ATR spectrum (cm^{-1}): 3256 (N-H-pyrrole), 2975 (C-H-pyrrole), 1734 (C=O-allylic ketone), 1658 (N-N-oxadiazole) 1462 (C=C-ethylene), 1251 (C-O-oxadiazole), 1060 (C-N-pyrrole), 792 (C-H-pyrrole), 744 (C-Br-bromo pyrrole); ^{1}H-NMR (400 MHz, $CDCl_3$) δ (ppm) =5. 14 (s, 1-H, N-H-2-pyrrole), 6.24 (s, 1-H, C-H-2-pyrrole), 6.69 (s, 1-H,C-H-1-ethylene), 7.56 (s, 1-H, C-H-1-ethylene); MS(ESI), *M/Z*: 346.96 (Molecular ion Peak).

(E)-3-(4,5-dichloro-1H-pyrrol-2-yl)-1-(5-phenyl-1,3,4-oxadiazolyl)prop-2-en-1-one(OP2)

Percentage of product yield: 71%; M.P(°C): 138-140; IR-ATR spectrum (cm^{-1}): 3362 (N-H-pyrrole), 3075 (C-H-pyrrole), 1724 (C=O-allylic ketone), 1671 (N-N-oxadiazole) 1472 (C=C-ethylene), 1351 (C-O-oxadiazole), 1070 (C-N-pyrrole, oxadiazole), 698 (C-H-pyrrole), 728 (C-Cl-chloro pyrrole); ^{1}H-NMR specrum (400 MHz, $CDCl_3$) δ (ppm)=5.21 (s, 1H, N-H-2-pyrrole), 6.26 (s, 1H, C-H-2-pyrrole), 6.77 (s,1-H,C-H-1-ethylene),7.44 (s,1-H,CH-1-ethylene); MS(ESI) *M/Z*: 258.06 (Molecular ion Peak).

(E)-3-(4,5-dibromo-1H-pyrrol-2-yl)-1-(5-phenyl-1,3,4-oxadiazolyl)prop-2-en-1-one(OP3)

Percentage of product yield: 69%; M.P(°C): 152;154; IR-ATR spectrum (cm^{-1}): 3241 (N-H-pyrrole), 2985 (C-H-pyrrole), 1725 (C=O-allylic ketone), 1652 (N-N-oxadiazole), 1480 (C=C-ethyelene), 1231 (C-O-oxadiazole), 1050 (C-N-pyrrole oxadiazole), 645 (C-H-pyrrole), 782 (C-Cl-chloro pyrrole); ^{1}H-NMR (400 MHz, $CDCl_3$-d_6) δ (ppm)=4. 99 (s, 1H, NH), 6.05 (s, 1-H, C-H) 7.54 (s, 1-H, C-H-ethylene), 6.57 (s, 1-H,C-H), 7.12 (s,1-H, C-H-Benzene), 7.32 (s,1-H, C-H-Benzene), 7.48 (s,1-H, C-H-Benzene), 7.54 (s, 1-H, C-H-1-ethylene); MS(ESI) *M/Z*: 423.06 (Molecular ion Peak).

(E)-3-(4,5-dichloro-1H-pyrrol-2-yl)-1-(5-phenyl-1,3,4-oxadiazolyl)prop-2-en-1-one(OP4)

Percentage of product yield: 70%; M.P (°C): 148;150; IR-ATR spectrum (cm^{-1}): 3376 (N-H-pyrrole), 3055 (C-H-pyrrole), 1744 (C=O-allylic ketone), 1648 (N-N-oxadiazole), 1350 (C=C-ethylene), 1145 (C-O-oxadiazole), 1040 (C-N-pyrrle, oxadizole), 752 (C-H-pyrrole), 741 (C-Cl-chloro pyrrole); ^{1}H-NMR (400 MHz, CDCl$_3$-d_6) δ (ppm)=5. 13 (s, 1-H, N-H-2-pyrrole), 6.06 (s, 1-H, C-H-2-pyrrole), 6.63 (s, 1-H,C-H-1-ethylene), 7.22 (s, 1-H, C-H-1-benzene) 7.32 (s,1-H, C-H-Benzene), 7.48 (s,1H, C-H-Benzene), 7.49 (s, 1-H, C-H-1-ethylene); MS(ESI) *M/Z*: 334.16 (Molecular ion Peak).

(E)-3-(4,5-dibromo-1H-pyrrol-2-yl)-1-(5-methyl-1,3,4-oxadiazolyl)prop-2-en-1-one(OP5)

Percentage of product yield: 68%; M.P(°C): 147;149; IR-ATR spectrum (cm^{-1}): 3351 (N-H-pyrrole), 3065 (C-H-pyrrole), 2835 (C-H-Methyl), 1734 (C=O-allylic ketone), 1659 (N-N-oxadiazole), 1450 (C=C-ethylene), 1341 (C-O-oxadiazole), 1080 (C-N-pyrrole, oxadiazole), 678 (C-H-pyrrole), 748 (C-Br-bromo pyrrole); ^{1}H-NMR (400 MHz, CDCl$_3$) δ (ppm)=2.35 (s, 3H, CH$_3$), 5. 24 (s, 1H, NH-2-pyrrole), 6.15 (s, 1H, C-H-2-pyrrole), 6.57 (s, 1-H,C-H-1-ethylene), 7.53 (s, 1-H, C-H-1-ethylene); MS(ESI), *M/Z*: 360.99 (Molecular ion Peak).

(E)-3-(4,5-dichloro-1H-pyrrol-2-yl)-1-(5-methyl-1,3,4-oxadiazolyl)prop-2-en-1-one(OP6)

Percentage of product yield: 72%; M.P(°C): 145-146; IR-ATR spectrum (cm^{-1}): 3344 (N-H-pyrrole), 3023 (C-H-pyrrole), 2825 (C-H-Methyl), 1739 (C=O-allylic ketone), 1651 (N-N-oxadiazole), 1350 (C=C-ethylene), 1251 (C-O-oxadiazole), 1040 (C-N-pyrrole, oxadiazole), 748 (C-H-pyrrole), 791 (C-Cl-chloro pyrrole); ^{1}H-NMR (400 MHz, CDCl$_3$) δ (ppm)=2.33 (s, 3H, CH3), 5. 11 (s, 1H, NH-2-pyrrole), 6.16 (s, 1H, C-H-2-pyrrole), 6.68 (s, 1H,C-H-1-ethylene), 7.56 (s, 1-H, C-H-1-ethylene); MS(ESI) *M/Z*: 272.09 (Molecular ion Peak).

(E)-1-(5-amino-1,3,4-oxadiazolyl)-3-(4,5-dibromo-1H-pyrrol-2-yl)prop-2-en-1-one(OP7)

Percentage of product yield: 74%; M.P(°C): 143-144; IR-ATR spectrum (cm^{-1}): 3465 (N-H-amino) 3391 (N-H-pyrrole), 3010 (C-H-pyrrole), 1726 (C=O-allylic ketone), 1654 (N-N-oxadiazole), 1480 (C=C-ethylene), 1241 (C-O-oxadiazole), 1070 (C-N-pyrrole, oxadiazole), 878 (C-H-pyrrole), 778 (C-Br-bromo pyrrole); ^{1}H-NMR(400 MHz, CDCl$_3$) δ (ppm)= 4.04 (s, 2H, NH2), 5. 03 (s, 1H, NH-2-pyrrole), 6.16 (s, 1-H, C-H-2-pyrrole), 6.66 (s, 1-H,C-H-1-ethylene), 7.52 (s, 1-H, C-H-1-ethylene); MS(ESI) *M/Z*: 361.98 (Molecular ion Peak).

(E)-1-(5-amino-1,3,4-oxadiazolyl)-3-(4,5-dichloro-1H-pyrrol-2-yl)prop-2-en-1-one(OP8)

Percentage of product yield: 79%; M.P(°C): 141-242; IR-ATR spectrum (cm^{-1}): 3465 (N-H-amino), 3321 (N-H-pyrrole), 3045 (C-H-pyrrole), 1749 (C=O-allylic ketone), 1626 (N-N-oxadiazole), 1550 (C=C-ethylene), 1351 (C-O-oxadiazole), 1041 (C-N-pyrrole, oxadiazole), 846 (C-H-pyrrole), 764 (C-Cl-chloro pyrrole); ^{1}H-NMR (400 MHz, CDCl$_3$) δ (ppm)=4.02 (s, 2-H, NH2), 5. 07 (s, 1H, NH-2-pyrrole), 6.19 (s, 1H, C-H-2-pyrrole), 6.69 (s, 1-H,C-H-1-ethylene), 7.59 (s, 1-H, CH-1-ethylene); MS(ESI) *M/Z*: 273.08 (Molecular ion Peak).

(E)-3-(4,5-dibromo-1H-pyrrol-2-yl)-1-(5-hydroxy-1,3,4-oxadiazolyl)prop-2-en-1-one(OP9)

Percentage of product yield: 81%; M.P(°C): 139;140; IR-ATR spectrum (cm^{-1}): 3365 (O-H-hydroxy), 3221 (N-H-pyrrole), 2945 (C-H-pyrrole), 1743 (C=O-allylic ketone), 1638 (N-N-oxadiazole), 1570 (C=C-ethylene), 1161 (C-O-oxadiazole), 1010 (C-N-pyrrole, oxadiazole), 892 (C-H-pyrrole), 708 (C-Br-bromo pyrrole); ^{1}H-NMR (400 MHz, CDCl$_3$) δ (ppm)=4.47 (s, 1-H, OH), 5. 09 (s, 1-H, NH-2-pyrrole), 6.17 (s, 1-H, C-H-2-pyrrole), 6.65 (s, 1-H,C-H-1-ethylene), 7.59 (s, 1-H, C-H-1-ethylene); MS(ESI) *M/Z*: 362.96 (Molecular ion Peak).

(E)-3-(4,5-dichloro-1H-pyrrol-2-yl)-1-(5-hydroxy-1,3,4-oxadiazolyl)prop-2-en-1-one(OP10)

Percentage of product yield: 86%; M.P(°C): 137-138; IR-ATR spectrum (cm^{-1}): 3435 (O-H-hydroxy), 3331 (N-H-pyrrole), 3095 (C-H-pyrrole), 1738 (C=O-allylic ketone), 1656 (N-N-oxadiazole), 1545 (C=C-ethylene), 1211 (C-O-oxadiazole), 1049 (C-N-pyrrole, oxadiazole), 869 (C-H-pyrrole), 787 (C-Cl-chloro pyrrole); ^{1}H-NMR (400 MHz, CDCl$_3$) δ (ppm)=4.49 (s, 1-H, OH), 5. 04 (s, 1-H, N-H-2-pyrrole), 6.13 (s, 1-H, C-H-2-pyrrole), 6.63 (s, 1-H,C-H-1-ethylene), 7.58 (s, 1-H, C-H-1-ethylene); MS(ESI) *M/Z*: 316.1 (Molecular ion Peak).

(E)-3-(4,5-dibromo-1H-pyrrol-2-yl)-1-(5-mercapto-1,3,4-oxadiazolyl)prop-2-en-1-one(OP11)

Percentage of product yield: 91%; M.P(°C): 149-151; IR-ATR (cm^{-1}): 3231 (N-H-pyrrole), 3099 (C-H-pyrrole), 2628 (S-H-Thio), 1724 (C=O-allylic ketone), 1638 (N-N-oxadiazole), 1487 (C=C-ethylene), 1165 (C-O-oxadiazole), 1037 (C-N-pyrrole, oxadiazole), 782 (C-H-pyrrole), 772 (C-Br-bromo pyrrole); ^{1}H-NMR (400 MHz, CDCl$_3$) δ (ppm)=2.99 (s, 1-H, S-H), 5. 10 (s, 1-H, N-H-2-pyrrole), 6.21 (s, 1-H, C-H-2-pyrrole), 6.72 (s, 1-H,C-H-1-ethylene), 7.61 (s, 1-H, C-H-1-ethylene); MS(ESI) *M/Z*: 379.03 (Molecular ion Peak).

(E)-3-(4,5-dichloro-1H-pyrrol-2-yl)-1-(5-mercapto-1,3,4-oxadiazolyl)prop-2-en-1-one(OP12)

Percentage of product yield: 92%; M.P(°C): 148-150; IR-ATR spectrum (cm^{-1}): 3381 (N-H-pyrrole), 3065 (C-H-pyrrole), 2628 (S-H-Thio), 1734 (C=O-allylic ketone), 1629 (N-N-oxadiazole), 1450 (C=C-ethylene), 1341 (C-O-oxadiazole), 135 (C-N-oxadiazole-), 658 (C-H-pyrrole), 748 (C-Cl-dichloro pyrrole); ^{1}H-NMR (400 MHz, CDCl$_3$) δ (ppm)=3.03 (s, 1-H, S-H), 4.99 (s, 1-H, N-H-2-pyrrole), 6.08 (s, 1-H, C-H-2-pyrrole), 6.57 (s, 1-H,C-H-1-ethylene), 7.51 (s, 1-H, C-H-1-ethylene); MS(ESI) *M/Z*: 290.13 [Molecular ion Peak].

(E)-3-(4,5-dibromo-1H-pyrrol-2-yl)-1-(5-ethyl-1,3,4-oxadiazolyl)prop-2-en-1-one(OP13)

Percentage of product yield: 76%; M.P(°C):161-163; IR-ATR spectrum (cm^{-1}): 3261 (N-H-pyrrole), 3036 (C-H-pyrrole), 2865 (C-H-ethyl) 1729 (C=O-allylic ketone), 1637 (N-N-oxadiazole), 1330 (C=C-ethylene), 1291 (C-O-oxadiazole,), 1090 (C-N-oxadiazole), 658 (C-H-pyrrole), 748 (C-Br-bromo pyrrole); ^{1}H-NMR (400 MHz, CDCl$_3$) δ (ppm)=1.25 (d, 3-H, CH$_3$-methyl) 2. 59 (q, 2-H, CH$_2$-methylene), 5. 03 (s, 1-H, N-H-2-pyrrole), 6.06 (s, 1-H, C-H-2-pyrrole), 6.63 (s, 1H,C-H-1-ethylene), 7.56 (s, 1-H, C-H-1-ethylene); MS (ESI) *M/Z*: 375.02 (Molecular ion Peak).

(E)-3-(4,5-dichloro-1H-pyrrol-2-yl)-1-(5-ethyl-1,3,4-oxadiazolyl)prop-2-en-1-one(OP14)

Percentage of product yield: 75%; M.P(°C): 161-163; IR-ATR spectrum (cm^{-1}): 3242 (N-H-pyrrole), 3077 (C-H-pyrrole), 2885 (C-H-ethyl), 1732 (C=O-allylic ketone),1624 (N-N-oxadiazole) 1494 (C=C-ethylene), 1151 (C-O-oxadiazole), 1064 (C-N-oxadiazole), 690 (C-H-pyrrole), 626 (C-Cl-dichloro pyrrole); -NMR (^{1}H) (400 MHz, CDCl$_3$) δ (ppm) =1.23 (d, 3-H, CH$_3$-methyl) 2. 57 (q, 2-H, CH$_2$-methylene), 5. 23 (s, 1-H, N-H-2-pyrrole), 6.23 (s, 1-H, C-H-2-pyrrole), 6.26 (s, 1-H,C-H-1-ethylene), 7.59 (s, 1-H, C-H-1-ethylene); MS (ESI) *M/Z*:286.11 (Molecular ion Peak).

(E)-3-(4,5-dibromo-1H-pyrrol-2-yl)-1-(5-(hydroxymethyl)-1,3,4-oxadiazolyl)prop-2-en-1-one(OP15)

Percentage of product yield: 64%; M.P(°C): 159-160; IR-ATR spectrum (cm^{-1}): 3412 (O-H-hydroxymethyl), 3351 (N-H-pyrrole), 3065 (C-H-pyrrole), 1739 (C=O-allylic ketone), 1648 (N-N-oxadiazole), 1450 (C=C-ethylene), 1351 (C-O-oxadiazole), 1080 (C-N-pyrrole, oxadiazole), 848 (C-H-pyrrole), 748 (C-Br-bromo pyrrole); ^{1}H-NMR (400 MHz, CDCl$_3$) δ (ppm)=2.02 (t, 1-H, OH) 4. 77 (s, 2-H, CH$_2$-methylene), 5. 12 (s, 1-H, NH-2-pyrrole), 6.18 (s, 1-H, C-H-2-pyrrole), 6.66 (s, 1-H,C-H-1-ethylene), 7.58 (s, 1-H, C-H-1-ethylene); MS (ESI) *M/Z*:361.98 (Molecular ion Peak).

(E)-3-(4,5-dichloro-1H-pyrrol-2-yl)-1-(5-(hydroxymethyl)-1,3,4-oxadiazolyl)prop-2-en-1-one(OP16)

Percentage of product yield: 63%; M.P(°C): 158-159; IR-ATR spectrum (cm^{-1}): 3432 (O-H-hydroxy methyl), 3358 (N-H-pyrrole), 3065 (C-H-pyrrole), 1747 (C=O), 1648 (N-N-oxadiazole), 1458 (C=C ethylene), 1341 (C-O-oxadiazole), 1080 (C-N-pyrrole), 678 (C-H), 748 (C-Br); ^{1}H-NMR (400 MHz, $CDCl_3$) δ (ppm)=2.05 (t, 1-H, OH) 4. 76 (s, 2-H, CH_2-methylene), 5. 0 (s, 1-H, NH-2-pyrrole), 6.08 (s, 1-H, C-H-2-pyrrole), 6.59 (s, 1-H,C-H-1-ethylene), 7.59 (s, 1-H, CH-1-ethylene); MS(ESI) *M/Z*: 288.09 (Molecular ion Peak)

(E)-N-(5-(3-(4,5-dibromo-1H-pyrrol-2-yl)acryloyl)-1,3,4-oxadiazolyl) acetamide(OP17)

Percentage of product yield: 73%; M.P(°C): 171-172; IR-ATR spectrum (cm^{-1}): 3652 (N-H-acetamide), 3359 (N-H-pyrrole), 3068 (C-H-pyrrole), 1734 (C=O-allylic ketone), 1648 (N-N-oxadiazole), 1456 (C=C-ethylene), 1361 (C-O-oxadiazole), 1080 (C-N-pyrrole, oxadiazole), 834 (C-H-pyrrole), 748 (C-Br-bromo pyrrole); NMR (^{1}H) (400 MHz, $CDCl_3$) δ (ppm)=2.04 (s, 3-H, CH_3), 4.72 (s, 2-H, CH_2-methylene), 5.08 (s, 1-H, NH-2-pyrrole), 6.17 (s, 1-H, C-H-2-pyrrole), 6.71 (s, 1-H,C-H-1-ethylene), 7.67 (s, 1-H, C-H-1-ethylene), 8.04 (s,1H, N-H-sec amide); MS(ESI) *M/Z*: 404.01 (Molecular ion Peak)

(E)-N-(5-(3-(4,5-dichloro-1H-pyrrol-2-yl)acryloyl)-1,3,4-oxadiazolyl) acetamide(OP18)

Percentage of product yield: 72%; M.P(°C): 169;170; IR-ATR spectrum (cm^{-1}): 3641 (N-H-acetamide), 3461 (N-H-pyrrole), 2985 (C-H-pyrrole), 1734 (C=O-allylic ketone), 1678 (N-N-oxadiazole), 1571 (C=C-ethylene), 1231 (C-O-oxadiazole), 1010 (C-N-oxadiazole, pyrrole), 740 (C-H-pyrrole), 735 (C-Cl); ^{1}H-NMR (400 MHz, $CDCl_3$) δ (ppm)=2.03 (s, 3-H, CH_3) 4.75 (s, 2H, CH_2-methylene), 5.12 (s, 1H, NH-2-pyrrole), 6.21 (s, 1H, C-H-2-pyrrole), 6.57 (s, 1-H,C-H-1-ethylene), 7.62 (s, 1-H, CH-1-ethylene), 8.12 (s,1-H, NH-sec amide); MS(ESI) *M/Z*:315.11 (Molecular ion Peak)

(E)-5-(3-(4,5-dibromo-1H-pyrrol-2-yl)acryloyl)-1,3,4-oxadiazolyl acetate(OP19)

Percentage of product yield: 70%; M.P(°C): 162;164; IR-ATR spectrum (cm^{-1}): 3265 (N-H-pyrrole), 3035 (C-H-pyrrole), 1759 (C=O-acetate), 1734 (C=O-allylic ketone), 1628 (N-N-oxadiazole), 1525 (C=C-ethylene), 1231 (C-O-oxadiazole), 1040 (C-N-pyrrole, oxadiazole), 838 (C-H-pyrrole), 783 (C-Br); ^{1}H-NMR (400 MHz, $CDCl_3$) δ (ppm)=2.06 (s, 3-H, CH_3), 5.14 (s, 1-H, NH-2-pyrrole), 6.17 (s, 1-H, C-H-2-pyrrole), 6.69 (s, 1-H,C-H-1-ethylene), 7.52 (s, 1-H, C-H-1-ethylene); MS(ESI) *M/Z*: 405.00 (Molecular ion Peak).

(E)-5-(3-(4,5-dichloro-1H-pyrrol-2-yl)acryloyl)-1,3,4-oxadiazolyl acetate(OP20)

Percentage of product yield: 73%; M.P(°C): 158;159; IR-ATR spectrum (cm^{-1}): 3452 (N-H-pyrrole), 3015 (C-H-pyrrole), 1759 (C=O-acetate), 1742 (C=O-allylic ketone), 1652 (N-N-oxadiazole), 1520 (C=C-ethylene), 1111 (C-O-oxadizole), 1030 (C-N-pyrrole, oxadiazole), 642 (C-H-pyrrole), 630 (C-Cl); ^{1}H-NMR (400 MHz, $CDCl_3$) δ (ppm)=2.07 (s, 3-H, CH_3), 5. 01 (s, 1-H, N-H-2-pyrrole), 6.03 (s, 1-H, C-H-2-pyrrole), 6.61 (s, 1-H,C-H-1-ethylene), 7.58 (s, 1-H, C-H-1-ethylene); MS(ESI) *M/Z*: 316.10 (Molecular ion Peak).

(E)-3-(4,5-dibromo-1H-pyrrol-2-yl)-1-(5-methoxy-1,3,4-oxadiazolyl) prop-2-en-1-one(OP21)

Percentage of product yield: 67%; M.P(°C).: 144;145; IR-ATR spectrum (cm^{-1}): 3231 (N-H-pyrrole), 3045 (C-H-pyrrole), 1736 (C=O-allylic ketone), 1656 (N-N-oxadiazole), 1582 (C=C), 1191 (C-O-oxadiazole), 1260 (C-O-C-methoxy), 1050 (C-N-pyrrole, oxadiazole), 864 (C-H-pyrrole), 768 (C-Br): ^{1}H-NMR (400 MHz, $CDCl_3$) δ (ppm)=3.76 (s, 3-H, CH_3), 5. 21 (s, 1-H, NH-2-pyrrole), 6.22 (s, 1-H, C-H-2-pyrrole), 6.70 (s, 1-H,C-H-1-ethylene), 7.49 (s, 1-H, C-H-1-ethylene); MS(ESI) *M/Z*: 376.99 (Molecular ion Peak).

(E)-3-(4,5-dichloro-1H-pyrrol-2-yl)-1-(5-methoxy-1,3,4-oxadiazolyl) prop-2-en-1-one(OP22)

Percentage of product yield: 62%; M.P(°C) 142-143; IR-ATR spectrum (cm^{-1}): 3361 (N-H-pyrrole), 3055 (C-H-pyrrole), 1739 (C=O-allylic ketone), 1638 (N-N-oxadiazole), 1490 (C=C-ethylene), 1251 (C-O-oxadiazole), 1240 (C-O-C-methoxy), 1020 (C-N-pyrrole, oxadiazole), 828 (C-H-pyrrole), 688 (C-Cl); ^{1}H-NMR (400 MHz, $CDCl_3$) δ (ppm)=3.65 (s, 3H, CH_3), 4.98 (s, 1H, NH-2-pyrrole), 6.01 (s, 1-H, C-H-2-pyrrole), 6.54 (s, 1-H,C-H-1-ethylene), 7.66 (s, 1-H, C-H-1-ethylene); MS(ESI) *M/Z*:288.09 (Molecular ion Peak).

DISCUSSION

Chemistry

Scheme 1 depicts the chemical process used to synthesize the target compounds (OP1–OP22). First, using somewhat modified techniques from previously published methods, molecules 4,5-dibromopyrrole, 4,5 dichloropyrrole (1a-1b), and 2-substituted 1,3,4 oxadiazole 5-ethanone (2a-2k) were synthesized [24]. Their nuclear magnetic resonance spectrum for to check numbers of hydrogen revealed a peak in singlet at around δ 5.0 and 6.1 ppm for N-H group (pyrrole-secondary amine) protons in pyrrole, whereas their IR spectra revealed the presence of a distinctive band at about 3456 cm^{-1} attributable to the pyrrole NH (amino) group and C=O allylic carbonyl liker stretching frequency at about 1697 cm^{-1}. A D2O exchange experiment was used to confirm the existence of these chemical compounds. By treating 4,5-dibromo pyrrole (1a) or 4,5-dichloro pyrrole (1b) with the proper 2-substituted 1,3,4-oxadizole 5-ethanone using a traditional base-catalyzed Claisen–Schmidt condensation, the essential intermediate α, β-unsaturated ketones (OP1–OP22) were created. The bridge between pyrrole and oxadiazole, i.e., alkene (C=C) group of allylic ketone, was identified as the source of a new band at 1430–1570 cm^{-1} in the compounds' (OP1–OP22) infrared spectra. Furthermore, the completion of the Claisen–Schmidt condensation processes was confirmed by the presence of two peaks of hydrogens with a geometrical E isomeric coupling constant (J =6 Hz) at δ 6.67 and 7.54 ppm, which are methylene groups. The target compounds are produced by the reaction of dihalogenated pyrrole with 2-substituted oxadiazole 5-ethanone in the presence of sodium hydroxide and ethanol with reflux for 2 h. FTIR, NMR, and mass spectroscopy were among the various spectroscopic methods used to clarify the produced chemicals.

These compounds' FTIR spectra revealed a strong peak with stretching vibration for the C=C stretch occurring between 1535 and 1560 cm^{-1}, an N-H vibration band appearing between 3435 and 3456 cm^{-1}, and an allylic ketone exhibiting a C=O absorption band between 1691 and 1670 cm^{-1}. The NMR spectrum revealed a singlet at approximately δ 5.1–5.3 ppm for the pyrrole proton. Between 6.6 and 7.65 ppm, the ethylene protons showed up as two singlets. Ultimately, mass spectrum data verified the production of these molecules. The synthetic strategy for the molecular hybrid of pyrrole with oxadiazole includes three steps: Halogenation of pyrrole, Synthesis of different derivative oxadiazole derivatives, and final Claisen–Schmidt condensation of pyrrole and oxadiazole for the molecular hybrid.

MABA assay for antimycobacterial activity

Using the MABA assay, the novel molecular hybrids of pyrrole and oxadiazole (OP1–OP22) were evaluated against the antibacterial-sensitive mycobacterial cell (MTB) strain H37Rv [25,26]. Every synthetic molecular hybrid of pyrrole and oxadiazole has its MIC value determined, which is the lowest concentration of the compound needed to completely inhibit bacterial growth. As reference medications for comparison, isoniazid, pyrazinamide, rifampin, and streptomycin were used. Table 1 summarizes the outcomes of antitubercular action. Based on the results, it was observed that, in comparison to the reference

Table 1: Physiochemical characterization data of synthesized derivatives OP1–OP22 and biological evaluation against MTB H37Rv

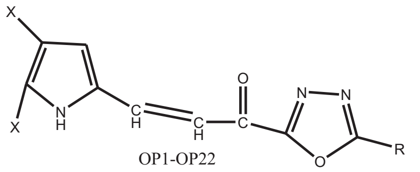

OP1-OP22

X-Pyrrole Substituents: X- Br, Cl

R- Oxadiazole Substituents-R-H, C_6H_5, CH_3, NH_2,OH, SH, C_2H_5, CH_2OH, $NHCOCH_3$, $OCOCH_3$, OCH_3

Comp.	*Pyrrole substituents*	*Oxadiazole Substituents*	% Yield	Melting point (°C)[a]	Docking Score (A°)	MIC (μM)[b]	Rf value[c]
OP1	Br	H	75	142–144	−7.5	25.0	0.53
OP2	Cl	H	71	138–140	−7.8	6.25	0.56
OP3	Br	C_6H_5	69	152–154	−10.1	3.12	0.45
OP4	Cl	C_6H_5	70	148–150	−10.1	6.25	0.50
OP5	Br	CH_3	68	147–149	−8.4	25.0	0.49
OP6	Cl	CH_3	72	145–146	−8.3	6.25	0.51
OP7	Br	NH_2	74	143–144	−8.3	25.0	0.58
OP8	Cl	NH_2	79	141–142	−8.3	25.0	0.24
OP9	Br	OH	81	139–140	−8.4	12.5	0.88
OP10	Cl	OH	86	137–138	−8.4	12.5	0.87
OP11	Br	SH	91	149–151	−8.2	25.0	0.56
OP12	Cl	SH	92	148–150	−8.1	25.0	0.51
OP13	Br	C_2H_5	76	161–162	−8.5	12.5	0.49
OP14	Cl	C_2H_5	75	161–163	−8.4	12.5	0.51
OP15	Br	CH_2OH	64	159–160	−8.3	6.25	0.61
OP16	Cl	CH_2OH	63	158–159	−8.3	6.25	0.63
OP17	Br	$NHCOCH_3$	73	171–172	−9.5	12.5	0.71
OP18	Cl	$NHCOCH_3$	72	169–170	−9.5	12.5	0.56
OP19	Br	$OCOCH_3$	70	162–164	−9.2	12.5	0.55
OP20	Cl	$OCOCH_3$	73	158–159	−9.2	12.5	0.86
OP21	Br	OCH_3	67	144–145	−8.6	6.25	0.94
OP22	Cl	OCH_3	62	142–143	−8.5	6.25	0.85
Isoniazid	-	-	60	131–132	−6.2	1.12	0.45
Ciprofloxacin	-	-	70	161–162	−5.3	12.5	0.75

[a]The melting points were determined in open capillary tubes and are uncorrected [b]Minimum inhibitory concentration against MTB $H_{37}Rv$ calculated based on pink color intensity on ultraviolet spectrophotometer at 570 nm [c]Rf value calculated from TLC plate by distance traveled by solute divided by solvent, TLC: Mobile Phase: - *n*-Hexane (99.8%): Water (99.9%): Ethyl acetate (99.9%) [4:4:2] Isoniazid, Ciprofloxacin. MTB: *Mycobacterium tuberculosis*, MIC: Minimum inhibitory concentration, Rf: Retention factor

medication isoniazid (MIC=3.12 μM), the most active hybrid, OP3, showed MTB higher inhibition for antitubercular action at 3.12 μM. In contrast to ciprofloxacin (MIC=12.5 μM) and pyrazinamide (MIC=50 μM), three substances (OP2, OP4, OP15, OP16, OP21, and OP22) reduced MTB with a MIC value of 6.25 μM. It was discovered that six compounds – OP13, OP14, OP17, OP18, OP19, and OP20 – were equally potent to ciprofloxacin (12.5 μM). All of the compounds were determined to have greater potential than pyrazinamide when their activities were compared to that of pyrazinamide (50.0 μM). With the exception of OP3, 21 substances have demonstrated antitubercular efficacy; nevertheless, they are not as potent as isoniazid, the first-line antitubercular drug. In addition, the following characteristics of (E)-3-(4,5-dibromo-1H-pyrrol-2-yl's SAR. It has been demonstrated that -1-(5-phenyl-1,3,4-oxadiazol-2-yl)prop-2-en-1-one (OP3) significantly inhibits MTB. At 3.12 μM, the 4,5-dibromo pyrrole (OP3) molecule has a MIC of 3.12 μM, compared with the 4,5 dichloro derivative (OP4) with a MIC value of 6.25 μM, found to be potent, exhibiting that the bromo group at the 4, 5 position of the pyrrole increases antimycobacterial action. On the other hand, to see the effect of oxadiazole substituents, the phenyl substituent (OP3) compares with other oxadiazole substituents such as OH, NH_2, CH_3, $OCOCH_3$, $NHCOCOCH_3$, OCH_3, and SH, showing prominently greater activity, as stated in table 1. When H was added to the second position of the oxadiazole to replace the same phenyl group, $OCOCH_3$ and $NHCOCH_3$ (3,4-OCH_3) activities were found at 6.25 μM. When OH, $OCOCH_3$, and $NHCOCH_3$ were substituted for oxadiazole at position 2, a strong inhibitory action against MTB was seen at concentrations of 12.5 μM. The presence of electron-attracting groups SH and NH2 indicates that the activity has decreased to 25 μM. High activity (3.12 μM) was demonstrated by compounds OP3, which were changed at the 4,5 position of pyrrole and contained electron-withdrawing groups such as Br. Nonetheless, good action was demonstrated by the 5-chloro-substituted pyrrole (6.25 μM).

On the other hand, the 5-chloro-substituted pyrrole showed significant activity (6.25 μM).

The conclusion is that the biological activity is increased by the phenyl substitution at position 2 of oxadiazole and the bromo group at positions 4 and 5 of pyrrole. Other substituents such as OH, $OCOCH_3$, and $NHCOCH_3$ also increase the antitubercular activity, which is 12.50 μM, whereas the OCH_3 group at the oxadiazole 2 position increases biological activity, which is 6.25 μM. However, the antitubercular activity is reduced to 25 μM by the group SH, CH_3 at two pyrrole sites.

Lead-drug likeness parameters and the Lipinski's rule of five [25,26] are two new screening methods for comprehending molecular parameters that have emerged for checking drug compatibility with the body in recent years. The data obtained indicate that the majority of the synthesized compounds have better expected values for the hydrogen bond donor, polar surface area, and hydrogen bond acceptor. Lipinski's rule of five states that a biological therapeutic ligand should have a molecular weight of 500 or less, a number of hydrogen bond donor atoms of 5 or fewer, a number of hydrogen bond acceptor atoms of 10 or less (N or O), and a log p of no more than five. All new synthesized molecular hybrids were found to be good drug candidates as they all passed through the criteria of Lipinski's rule of five, as stated in table 2. Hence, the synthesized compounds generally comply with Lipinski's

Table 2: Drug likeness properties of molecular hybrid of pyrrole with oxadiazole (OP1–OP22)

Compounds	MW	Logp	NHDO	NHAC	TPSA	Compounds	MW	Logp	NHDO	NHAC	TPSA
Rule of five	≤500	≤5	≤10	≤5	60–120	OP13	375.02	2.69	1	4	71.28
OP1	346.96	1.45	1	4	71.28	OP14	286.11	2.08	1	4	71.78
OP2	258.06	0.84	1	4	71.78	OP15	376.99	1.52	2	5	92.02
OP3	423.06	3.5	1	4	71.28	OP16	288.09	0.92	2	5	92.01
OP4	334.16	2.89	1	4	71.78	OP17	404.01	1.33	2	5	100.88
OP5	360.99	2.12	1	4	71.78	OP18	315.11	0.73	2	5	100.88
OP6	272.09	1.51	1	4	71.78	OP19	405.00	2.01	1	5	98.08
OP7	361.98	1.62	2	4	97.8	OP20	316.1	1.41	1	5	98.08
OP8	273.08	1.02	2	4	97.8	OP21	376.99	2.3	1	5	81.01
OP9	362.96	2.04	2	5	92.01	OP22	288.09	1.69	1	5	81.01
OP10	274.06	1.43	2	5	92.02	INH	137.00	−0.969	4	3	68.01
OP11	379.03	2.61	1	4	110.58	Pyra	123.00	−0.711	4	2	68.87
OP12	290.13	2.01	1	4	110.58	Cipro	331.00	−0.701	6	2	74.56

MW: Molecular weight, LogP: Logarithm of partition coefficient between n-octanol and water, NHDO: Number of hydrogen bond donors, NHAC: Number of Hydrogen Accepters, TPSA: Topological polar surface area, docking score on MMAA4 pdb id 3HA7 in A°, 3HA7 in A°, INH: Isoniazid, Pyra: Pyrazinamide, Cipro: Ciprofloxacin, NHDO: Number of hydrogen donors

Table 3: Cell line cytotoxic assay of synthesized compounds against the human dermal fibroblast cell line

Compound	IC_{50} (μg/mL)	SI
OP3	20 μg/mL	4.65
OP4	40 μg/mL	3.32
OP6	30 μg/mL	3.11
OP15	50 μg/mL	4.12
OP16	60 μg/mL	5.23
OP21	30 μg/mL	3.35
OP22	30 μg/mL	4.45

Précised observation considered for SI and IC_{50} value. SI: Selectivity index

rule of five, which confirms that all possess properties conducive to oral bioavailability.

Cytotoxicity activity assay

The active compounds' *in vitro* cytotoxicity (IC_{20} ≤ 12.5 μg/ml Human Dermal Cell) was assessed using a 3-(4, 5-dimethylthiazo-2-yl)-2,5-diphenyl-tetrazolium bromide (MTT) cell proliferation assay against a normal human dermal fibroblast (HDF) cell line. Table 3 illustrates the inhibition of cell growth by the active chemicals at different concentrations dose graphically. The lack of general toxicity was demonstrated by the assay data, which showed that none of the active chemicals were harmful to healthy cells.

The IC_{50} values were calculated from the absorbance of a given concentration, and the lowest IC_{50} value was found for OP3 compounds, i.e., 20 μg/mL for the normal human dermal cell line, while the selectivity index was also more than 2.

CONCLUSION

A number of pyrroles with oxadiazole molecular hybrid derivatives (OP1–OP22) were designed and produced. The molecular docking of all hybrid molecules of pyrrole with oxadiazole was performed on the active site of the receptor, pdb code 3HA7. The MTT cell proliferation assay was used to evaluate for cytotoxicity against normal HDF cell lines, and all derived hybrid molecules (OP1–OP22) were subjected to *in vitro* antitubercular evaluation against MTB H37Rv. According to the molecular docking result data, OP3((E)-3-(4,5-dibromo-1H-pyrrol-2-yl)-1-(5-phenyl-1,3,4-oxadiazol-2-yl)prop-2-en-1-one) and OP4 (E)-3-(4,5-dichloro-1H-pyrrol-2-yl)-1-(5-phenyl-1,3,4-oxadiazol-2-yl)prop-2-en-1-one were been observed most potent compounds and *in vitro* MABA assay verified that OP3 is the most antitubercular compound as shown most potent action on mycobacterial strain H37Rv with MIC of 3.12 μM and selective index toward infected human dermal cell is more than 2. All selected potent derivatives were found to be safer. Therefore, a molecular combination of pyrrole and oxadiazole may be a feasible strategy for creating novel MTB inhibitory drugs.

ACKNOWLEDGMENT

The authors are grateful to the Principal, Annasaheb Dange College of B. Pharmacy, Ashta, for providing the necessary facilities for this research.

AUTHORS' CONTRIBUTIONS

GM designed synthetic compounds based on virtual screening and synthesized NCE based on prepared synthetic schemes. Characterization and biological evaluation, cytotoxicity, and ADME, Lipinski properties were performed by MS.

FUNDING

The author received funding for this research from Shivaji University, Kolhapur, under the research initiation scheme and grant no. SU/C& U. D. S/2024-25/09/1199, 20/12/2024.

CONFLICTS OF INTERESTS

The authors do not have any conflicts of interest.

CONTENT AVAILABILITY

All the data from the research will be available in the manuscript.

REFERENCES

1. World Health Organization. Global Tuberculosis Report 2024 and Global Tuberculosis Report; 2024. Available from: https://who.int [Last accessed on 2025 Aug 03].
2. Rabahi MF, Da Silva Júnior JL, Ferreira AC, Tannus-Silva DG, Conde MB. Tuberculosis treatment. J Bras Pneumol. 2017;43(6):472-86. doi: 10.1590/S1806-37562016000000388, PMID 29340497
3. Davies PD, Yew WW. Recent developments in the treatment of tuberculosis. Expert Opin Investig Drugs. 2003;12(8):1297-312. doi: 10.1517/13543784.12.8.1297, PMID 12882618
4. Tiberi S, Muñoz-Torrico M, Duarte R, Dalcolmo M, D'Ambrosio L, Migliori GB. New drugs and perspectives for new anti-tuberculosis regimens. Pulmonology. 2018;24(2):86-98. doi: 10.1016/j.rppnen.2017.10.009, PMID 29487031
5. Asgaonkar KD, Mote GD, Chitre TS. QSAR and molecular docking studies of oxadiazole-ligated pyrrole derivatives as enoyl-ACP (CoA) reductase inhibitors. Sci Pharm. 2013;82(1):71-85. doi: 10.3797/scipharm.1310-05, PMID 24634843
6. Kim H, Gu L, Yeo H, Choi U, Lee CR, Yu H, *et al*. Rapid assembly of pyrrole-ligated 1,3,4-oxadiazoles and excellent antibacterial activity of iodophenol substituents. Molecules. 2023;28(8):3638. doi: 10.3390/molecules28083638, PMID 37110872
7. Long L, Zhang H, Zhou Z, Duan L, Fan D, Wang R, *et al*. Pyrrole-containing hybrids as potential anticancer agents: An insight into current developments and structure-activity relationships. Eur J Med Chem. 2024;273:116470. doi: 10.1016/j.ejmech.2024.116470, PMID 38762915

8. Kumar G, Kumar R, Mazumder A, Salahuddin, Kumar U. 1,3,4-oxadiazoles as anticancer agents: A review. Recent Pat Anticancer Drug Discov. 2024;19(3):257-67. doi: 10.2174/1574892818666230727102928, PMID 37497702
9. Kumar Madugula A, Kiran B, Suresh Varma Dendukuri BN, Kishore TV, Srinivasa Rao P, Ranagaih G, *et al*. Synthesis, characterization, and evaluation of antioxidant, antimicrobial and drug likeness properties of indole containing 1,3,4-oxadiazoles. Results Chem. 2024;9:101664. doi: 10.1016/j.rechem.2024.101664
10. Abd El-Hameed RH, Sayed AI, Mahmoud Ali S, Mosa MA, Khoder ZM, Fatahala SS. Synthesis of novel pyrroles and fused pyrroles as antifungal and antibacterial agents. J Enzyme Inhib Med Chem. 2021;36(1):2183-98. doi: 10.1080/14756366.2021.1984904, PMID 34602000
11. Zidar N, Macut H, Tomašič T, Peterlin Mašič LP, Ilaš J, Zega A, *et al*. New N-phenyl-4,5-dibromopyrrolamides as DNA gyrase B inhibitors. MedChemComm. 2019;10(6):1007-17. doi: 10.1039/c9md00224c, PMID 31303999
12. Gao Q, Liu S, Wu X, Zhang J, Wu A. Direct annulation of hydrazides to 1,3,4-oxadiazoles via oxidative C(CO)-C(Methyl) bond cleavage of methyl ketones. Org Lett. 2015;17(12):2960-3. doi: 10.1021/acs.orglett.5b01241, PMID 26035338
13. Dhakshinamoorthy A, Alvaro M, Garcia H. Claisen-Schmidt condensation catalyzed by metal-organic frameworks. Adv Synth Catal. 2010;352(4):711-7. doi: 10.1002/adsc.200900747
14. Shafi SS, Rajesh R, Senthilkumar S. Synthesis and characterization of boc-protected thio-1,3,4-oxadiazol-2-yl derivatives. Int J Chem Res. 2021;5(3):5-10. doi: 10.22159/ijcr.2021v5i3.169
15. Kachkurea D, Dhawale SA, Tapadiya G, Pawar C, Bharad J. Synthesis and evaluation of diazo-triazole hybrid as anti-tubercular agents. Int J Chem Res. 2025;9(4):34-9.
16. Sunil D, D'Almeida L, Kini SG, Rama M. Synthesis of quinolinyl-oxadiazole as a potent antibacterial agent and sa-fabi inhibitor. Int J Pharm Pharm Sci. 2015;7(8):105-9.
17. Joshi SD, Dixit SR, Kirankumar MN, Aminabhavi TM, Raju KV, Narayan R, *et al*. Synthesis, antimycobacterial screening and ligand-based molecular docking studies on novel pyrrole derivatives bearing pyrazoline, isoxazole and phenyl thiourea moieties. Eur J Med Chem. 2016;107:133-52. doi: 10.1016/j.ejmech.2015.10.047, PMID 26580979
18. Biradar SM, Mote GD, Asgaonkar KD, Chitre TS. Synthesis, docking and biological evaluation of pyrrole-2-carbohydrazide derivatives. Pharm Chem. 2015;7(2):153-9.
19. Franzblau SG, Witzig RS, McLaughlin JC, Torres P, Madico G, Hernandez A, *et al*. Rapid, low-technology MIC determination with clinical *Mycobacterium tuberculosis* isolates by using the microplate alamar blue assay. J Clin Microbiol. 1998;36(2):362-6. doi: 10.1128/jcm.36.2.362-366.1998, PMID 9466742
20. Meyer K, Rajanahalli P, Ahamed M, Rowe JJ, Hong Y. ZnO nanoparticles induce apoptosis in human dermal fibroblasts via p53 and p38 pathways. Toxicol *In Vitro*. 2011;25(8):1721-6. doi: 10.1016/j.tiv.2011.08.011, PMID 21903158
21. Mosmann T. Rapid colorimetric assay for cellular growth and survival: Application to proliferation and cytotoxicity assays. J Immunol Methods. 1983;65(1-2):55-63. doi: 10.1016/0022-1759(83)90303-4, PMID 6606682
22. Trott O, Olson AJ. AutoDock Vina: Improving the speed and accuracy of docking with a new scoring function, efficient optimization, and multithreading. J Comput Chem. 2010;31(2):455-61. doi: 10.1002/jcc.21334, PMID 19499576
23. O'Boyle NM, Banck M, James CA, Morley C, Vandermeersch T, Hutchison GR. Open babel: An open chemical toolbox. J Cheminform. 2011;3(1):33. doi: 10.1186/1758-2946-3-33, PMID 21982300
24. RCSB Protein Data Bank. PDB ID: 3H7A; 2024. Available from: https://www.rcsb.org/structure/3ha7 [Last accessed on 2025 Aug 01].
25. Lipinski CA, Lombardo F, Dominy BW, Feeney PJ. Experimental and computational approaches to estimate solubility and permeability in drug discovery and development settings. Adv Drug Deliv Rev. 2001;46(1-3):3-26. doi: 10.1016/s0169-409x(00)00129-0, PMID 11259830
26. Drug-Likeness and Molecular Property Prediction. Available from: https://www.swissadme.ch [Last accessed on 2025 Aug 03].